bioRxiv preprint doi: https://doi.org/10.1101/208405; this version posted October 24, 2017. The copyright holder for this preprint (which was not certified by peer review) is the author/funder. All rights reserved. No reuse allowed without permission.

RESEARCH

Distribution of Purines and Pyrimidines over miRNAs of Human, Gorilla and Chimpanzee

Jayanta Kumar Das[1*], Pabitra Pal Choudhury[1], Adwitiya Chaudhuri[2], Sk. Sarif Hassan[3] and Pallab Basu[4]

*Correspondence:
dasjayantakumar89@gmail.com
[1]Applied Statistics Unit, Indian Statistical Institute , 203, B. T. Road, West Bengal, 700108 India, Full list of author information is available at the end of the article
[†]Equal contributor

Abstract

Meaningful words in English need vowels to break up the sounds that consonants make. The Nature has encoded her messages in RNA molecules using only four alphabets A, U, C and G in which the nine member double-ring bases (adenine (A) and Guanine (G)) are purines, while the six member single-ring bases (cytosine (C) and uracil (U)) are pyrimidines. Four bases A, U, C and G of RNA sequences are divided into three kinds of classifications according to their chemical properties. One of the three classifications, the *purine-pyrimidine* class is important. In understanding the distribution (organization) of purines and pyrimidines over some of the non-coding regions of RNA, all miRNAs from three species of Family Hominidae (namely human, gorilla and chimpanzee) are considered. The distribution of purines and pyrimidines over miRNA shows deviation from randomness. Based on the quantitative metrics (fractal dimension, Hurst exponent, Hamming distance, distance pattern of purine-pyrimidine, purine-pyrimidine frequency distribution and Shannon entropy) five different clusters have been made. It is identified that there exists only one miRNA in human *hsa-miR-6124* which is purely made of purine bases only.

Keywords: miRNAs; Purines - Pyrimidines; Fractal dimension; Hurst exponent; Hamming distance; Shannon entropy; Clusters

AMS Subject Classification: 92B05 & 92B15

Introduction

The monomer units for forming the nucleic acid polymers deoxyribonucleic acid (DNA) and ribonucleic acid (RNA) are nucleotides which are grouped into three different classes based on their chemical properties, i.e., purine group R={A,G} and pyrimidine group Y={C,T/U}; amino group M={A,C} and keto group K={G,T/U}; strong H-bond group S={C,G} and weak H-bond group W={A,T/U} [1]. There are two kinds of nitrogen-containing bases - Purines and Pyrimidines, first isolated from hydrolysates of nucleic acids, were identified using classical methods of organic chemistry. An important contribution was made by Emil Fischer who must be credited with the earliest synthesis of purines (1897) [2]. Purines consist of a nine member double-ring (containing carbon and nitrogen) fused together, where as pyrimidines have a six member single-ring comprising of carbon and nitrogen. [3, 4]. The organization of purine-pyrimidine bases over RNA is crucial. Here we intend to understand the organization of the two chemical bases purine and pyrimidine over over some of the non-coding RNAs, *microRNA*.

bioRxiv preprint doi: https://doi.org/10.1101/208405; this version posted October 24, 2017. The copyright holder for this preprint (which was not certified by peer review) is the author/funder. All rights reserved. No reuse allowed without permission.

MicroRNAs (abbreviated miRNAs) contain about 18-25 ribonucleotides that can play important gene regulatory roles by pairing to the messages of protein-coding genes, to specify messenger RNA (mRNA) cleavage or repression of productive translation [5, 6, 7]. miRNA genes are one of the more abundant classes of regulatory genes in animals, estimated to comprise between 0.5 and 1 percent of the predicted genes in worms, flies, and humans, raising the prospect that they could have many more regulatory functions than those uncovered to date [8, 9]. The main function of miRNAs is to down-regulate gene expression [10]. A given miRNA may have hundreds of different mRNA targets, and a given target might be regulated by multiple miRNAs [11, 12, 13, 14, 15]. It is important to identify the miRNA targets accurately. miRNAs control gene expression by targeting mRNAs and triggering either translation repression or RNA degradation [16, 17]. Their aberrant expression may be involved in various human diseases, including cancer [18, 19, 20, 21, 22, 23, 24]. miRNA regulatory mechanisms are complex and there is still no high-throughput and low-cost miRNA target screening technique [25, 26, 27]. It is an well known fact that each miRNA is potentially able to regulate around 100 or more targeted mRNAs and 30% of all human genes are regulated by miRNAs [28].

In this article an attempt has been made to decipher the pattern of organization of purines and pyrimidines distributions over the miRNAs of the three species human, gorilla and chimpanzee. We desire to understand how the purine/pyrimidine bases are organized over the sequence and how much distantly the purine/pyrimidine bases can be placed over the sequence. Which one of these two type of chemical bases purine or pyrimidine dominates other in terms of their frequency density over the sequence is one of our prime aims to comprehend. A simple binomial distribution (i.e. location independent occurance of the bases) fails to describe the observed variation of Purine and Pyrimidine. This encourages us to look for further patterns. We investigate, the self-organization of the purine and pyrimidine bases for all the miRNAs of the three species human, gorilla and chimpanzee through the fractal dimension of the indicator matrix. The auto correlation of purine-pyrimidine bases over the miRNAs through the parameter Hurst exponent are determined and found many of the miRNAs have identical auto correlation even if their purine-pyrimidine organization is different. All the miRNAs are compared about their nearness based on their purine-pyrimidine distribution, Hamming distance is employed among all the miRNAs in understanding the nearness of purine-pyrimidine organization. The purine-pyrimidine distance patterns including the frequency distribution have been found for all the miRNAs for all three species. All possible distinct pattern of frequency distribution are determined for all the miRNAs of both the species. Here we wish to bring attention to the reader that through our investigation, the miRNA h1291, made of only purine bases is identified. There is no miRNA (human, gorilla and chimpanzee) which is absolutely made of pyrimidines.

Materials and Methods

Datasets

From the MiRBase (a miRNA database: **http://www.mirbase.org/**) [29], from the family Hominidae, total of 2588 mature miRNAs of human, 357 mature miRNAs

bioRxiv preprint doi: https://doi.org/10.1101/208405; this version posted October 24, 2017. The copyright holder for this preprint (which was not certified by peer review) is the author/funder. All rights reserved. No reuse allowed without permission.

of gorilla and 587 mature miRNAs of chimpanzee are taken. Each miRNA of human, gorilla and chimpanzee are encoded as numbers starting from $h1$ to the total number of sequences $h2588$ for miRNAs of human and same has been made for miRNAs of gorilla $g1$ to $g357$ and for miRNAs of chimpanzee $p1$ to $p587$ (*Additional file 1*). We then transform the miRNAs sequences (A, U, C, G) into binary sequences (1's and 0's) according to the following rules:

$$A/G \to 1;$$

$$U/C \to 0;$$

That means purine and pyrimidine nucleotide bases are encoded as 1 and 0 respectively into the transformed binary sequences of miRNAs. Therefore, presently we have three datasets of binary sequences of the three species human, gorilla and chimpanzee. All the computational codes are written in *Matlab R2016a* software.

Fractal Dimension of Indicator Matrices

Here we shall encode each binary sequences into its indicator matrices [30, 31]. It is noted that there are several other technique for finding fractal dimension anf self-organization structure of DNA sequences [32, 33]. Consider a set $\mathbf{S} = \{0, 1\}$ and an indicator function $f : \{0, 1\} \times \{0, 1\} \longleftrightarrow \{0, 1\}$ is defined as for all $(x, y) \in \mathbf{S} \times \mathbf{S}$,

$$f(x, y) = 1; x = y$$

$$f(x, y) = 0; x \neq y$$

This indicator function can be used to obtain the binary image of the binary sequence as a two dimensional dot-plot. The binary image obtained by this indicator matrix can be used to visualize the distribution of ones and zeros within the same binary sequence and some kind of auto-correlation between the ones and zeros of the same sequence. It can be easily drawn by assigning a black dot to 1 and a white dot to 0. An example of indicator matrix is shown in Fig. 1 for the binary sequence $Hsa-miR-576-3pMIMAT0004796$: 11110101111111100111100. From the indicator matrix, we can have an idea of the "fractal-like" distribution of ones and zeros (purines and pyrimidines). The fractal dimension for the graphical representation of the indicator matrix plots can be computed as the average of the number $p(n)$ of 1 in the randomly taken $n \times n$ minors of the $N \times N$ indicator matrix. Using $p(n)$, the fractal dimension (FD) is defined as

$$FD = \frac{1}{N} \sum_{n=2}^{N} \frac{logp(n)}{logn}$$

Hurst Exponent of Binary Sequences

The Hurst Exponent (HE) deciphers the long term memory of time series, i.e. the autocorrelation of the time series [34, 35, 36]. A value of $0 < HE < 0.5$ indicates

bioRxiv preprint doi: https://doi.org/10.1101/208405; this version posted October 24, 2017. The copyright holder for this preprint (which was not certified by peer review) is the author/funder. All rights reserved. No reuse allowed without permission.

a time series with negative autocorrelation and a value of $0.5 < HE < 1$ indicates a time series with positive autocorrelation. A value of $HE = 0.5$ indicates a true random walk, where it is equally likely that a decrease or an increase will follow from any particular value with higher values indicating a smoother trend and less roughness.

The Hurst exponent HE of a binary sequence $\{x_n\}$ is defined as $(\frac{n}{2})^{HE} = \frac{R(n)}{S(n)}$ where $S(n) = \sqrt{\frac{1}{n}\sum_i^n (x_i - m)}$ and $R(n) = maxY(i,n) - minY(i,n)$; $1 \leq i \leq n$ where $Y(i) = \sum_{j=1}^{i}(x_j - m)$ and $m = \sqrt{\frac{1}{n}\sum_{i=1}^{n} x_i}$

Hamming Distance of Binary Sequences

The Hamming Distance (HD) between two binary strings is the number of bits in which they differ [37, 38, 39]. Since length of the miRNAs might differ and hence a special care has been taken into consideration. Suppose there are two miRNAs S_m and S_n of length m and n respectively ($n > m$), then

$$HD(S_m, S_n) = min(hd(S_m, S_n))$$

where S_n of length n window is sliding over S_m from the left alignment to the right alignment and each time hamming distance (hd) is calculated, and finally minimum hd value is taken as hamming distance HD of two binary sequences.

For example, take two binary sequences $S_m = 010100$ and $S_n = 1101$, now sliding of S_n over S_m of length 4, from left to right alignment of these two sequences, we find the hamming distances are hd(**0101**00,**1101**)=1, hd(0**1010**0,**1101**)=3, hd(01**0100**,**1101**)=2, therefore we take $HD = 1$ (minimum) of these two binary sequences. Finding the minimum hamming distance of the two binary sequences says about the maximum similarity of two sequences over the distribution of purines and pyrimidines. The minimum value of $HD = 0$ when the pattern of length $min(m,n)$ of two binary sequences of miRNAs are exactly identical i.e. similar distribution of purines and pyrimidines over the miRNAs of the two sequences and the maximum value of $HD = min(m,n)$ when the pattern of length $min(m,n)$ of two binary sequences of miRNAs are exactly opposite i.e. completely dissimilar distribution of purines and pyrimidines over miRNAs two sequences.

Distance pattern of purine and pyrimidine over miRNAs

Here we are exploring the distance pattern of purines bases across the miRNAs human, gorilla and chimpanzee. How sparsely (closely) purine bases are placed over the miRNAs. So we found the distance (gap) between purine bases to the immediate next purine base over the miRNA sequences.

For example, take a transformed binary sequence $S_m = 110100111000001$, where 1 indicates the purines bases and 0 indicates pyrimidine bases in the sequence. From left to right the positions of 1's and 0's in serial is shown below. Now, form the distribution of 1's, we find the purine distances at 1 (two consecutive 1's at a distance of 1: 11), 2 (two consecutive 1's at a distance of 2: 101), 3 (two consecutive 1's at a distance of 3: 1001) and 6 (two consecutive 1's at a distance of

bioRxiv preprint doi: https://doi.org/10.1101/208405; this version posted October 24, 2017. The copyright holder for this preprint (which was not certified by peer review) is the author/funder. All rights reserved. No reuse allowed without permission.

6: 1000001). So, the distance pattern of purines over the sequence is [1 2 3 6] in order.

Positions	1	2	3	4	5	6	7	8	9	10	11	12	13	14	15
Sequence	1	1	0	1	0	0	1	1	1	0	0	0	0	0	1

Similar to the distance pattern of purine, the distance pattern of pyrimidine bases (0's) across the miRNAs also can be determined. The distance pattern of pyrimidines of the above sequence is [1 2 4] in order. Further the distance pattern of pyrimidines [1 **2** **4**] of a miRNA opens up a fact that there is at least one $1(= \mathbf{2} - 1)$ and at least one $3(= \mathbf{4} - 1)$ length purine blocks present in the miRNA. In the similar way, a distance pattern of purine triggers the presence of pyrimidine blocks in miRNAs.

Shannon entropy of miRNAs

The Shannon entropy (SE) is defined as the entropy of a Bernoulli process with probability p of one of two values [40, 41, 42]. It is defined as

$$SE = -\sum_{i=1}^{2} p_i log_2(p_i)$$

Here $p_1 = \frac{k}{2^l}$ and $p_2 = \frac{l-k}{2^l}$; here l is length of the binary string and k is the number of 1s in the binary string of length l.

The *Shannon entropy* is a measure of the uncertainty in a binary string. To put it intuitively, suppose $p = 0$. At this probability, the event is certain never to occur, and so there is no uncertainty at all, leading to an entropy of 0. If $p = 1$, the result is again certain, so the entropy is 0 here as well. When $p = 1/2$, the uncertainty is at a maximum; if one were to place a fair bet on the outcome in this case, there is no advantage to be gained with prior knowledge of the probabilities. In this case, the entropy is maximum at a value of 1 bit. Intermediate values fall between these cases; for instance, if $p = 1/4$, there is still a measure of uncertainty on the outcome, but one can still predict the outcome correctly more often than not, so the uncertainty measure, or entropy, is less than 1 full bit.

Results and Classifications of miRNAs

Deviation from randomness

A simple random binomial (p,q) model [43], where each entries can either be purine (or pyrimidine) with probability p (or $q = 1 - p$) fails to address the distribution of purine or pyrimidine over miRNAs. If we calculate the mean of the distribution from the sample and calculate the probability p, and if we calculate the probability p from the variance then we get different values. In all three species, the expected variances are significantly smaller than what we would have expected from the binomial distribution.

In human $p = 0.509$, chimpanzee $p = 0.505$, gorilla $p = 0.514$ from mean. Expected std = 2.327 (human),2.323 (chimpanzee), 2.322 (gorilla). Sample std = 3.35 (human), 2.78 (chimpanzee), 2.58 (gorilla).

bioRxiv preprint doi: https://doi.org/10.1101/208405; this version posted October 24, 2017. The copyright holder for this preprint (which was not certified by peer review) is the author/funder. All rights reserved. No reuse allowed without permission.

Classification Based on FDs of Indicator Matrices

The fractal dimension for each binary sequence of human, gorilla and chimpanzee miRNAs as entire data is given in the *Additional file 2 (sheet-1)*. Based on the fractal dimension, we have made classifications for the all the datasets of human, gorilla and chimpanzee. There are 10 clusters of miRNAs for the species human, gorilla and chimpanzee as shown in Table 1. The fractal dimensions including the histograms of all the miRNAs of human, gorilla and chimpanzee are plotted in the Fig. 2. Also a normal distribution fitting is also made as shown in Fig.3. The detail members (miRNAs) of the clusters for human, gorilla and chimpanzee are given in the *Additional file 2 (sheet-2)*.

It is observed that the FD of miRNAs of human lies in the interval $[1.51, 1.9]$ and the largest cluster(center at 1.60) contains 931 miRNAs whereas the FD of miRNAs of gorilla lies in the interval $[1.55, 1.864]$ which is contained in the interval $[1.51, 1.9]$ and the FD of miRNAs of chimpanzee lies in the interval $[1.54, 1.83]$ and the largest cluster (center at 1.58) contains 255 miRNAs. The largest cluster (center at 1.60) of miRNAs of gorilla contains 151 members. The centers of all the three largest clusters of miRNAs of human, gorilla and chimpanzee are approximately same which is a reflection of the fact that all these three species of the family *Hominidae* belong to the same family and are evolutionarily close. It is noted that there is no miRNAs of gorilla whose FD lies in between 1.76 and 1.84 whereas there are approximately 72 miRNAs of human and 7 miRNAs of chimpanzee whose FD lies in the said interval. There are clusters (for human, gorilla and chimpanzee) with largest centers among the other centers of the clusters contain 5, 2 and 3 members respectively.

Classification Based on HEs

For every sequence of miRNA of human, gorilla and chimpanzee, Hurst exponent are determined (*Additional file 3 (sheet-1)*) and then a classification is made based on the computed Hurst exponent for miRNAs of human, gorilla and chimpanzee, which is shown in Table 2. There are 10 clusters for all the species human, gorilla and chimpanzee miRNAs as shown in Table 2. The Hurst exponents and the histograms of all the miRNAs of human and gorilla are plotted in the Fig. 4. Also a normal distribution fitting is also made as shown in Fig.5. The detail members (miRNAs) of the clusters for human, gorilla and chimpanzee are given in the *Additional file 3 (sheet-2)*. The HE of miRNAs of human lies in the interval $[0.2659, 0.9639]$ and the largest cluster(center at 0.7197) contains 671 miRNAs whereas the HE of miRNAs of gorilla lies in the interval $[0.375, 0.964]$ and HE of miRNAs of chimpanzee in the interval $[0.2745, 0.9589]$. The largest cluster (center at 0.64) of miRNAs of gorilla contains 69 members and the same(center at 0.7194) contains 134 miRNAs of chimpanzee. The centers of the HE clusters in the case human and chimpanzee are close enough where as the center of the largest cluster of miRNAs of gorilla is significantly different from other two species unlike FD as stated in the above section. It interprets basically the long range autocorrelations of miRNAs of gorilla is different significantly from the miRNAs of human and chimpanzee. It also shows the evolutionary closeness of human and chimpanzee in comparison with other two possible pairs (chimpanzee, gorilla) and (human, gorilla).

bioRxiv preprint doi: https://doi.org/10.1101/208405; this version posted October 24, 2017. The copyright holder for this preprint (which was not certified by peer review) is the author/funder. All rights reserved. No reuse allowed without permission.

Classification Based on HDs

The detail pairs of miRNAs based on Hamming distances of human, gorilla and chimpanzee are given in the *additional file-4 (sheet-1)*, *additional file-4 (sheet-2)* and *additional file-4 (sheet-3)* respectively . We then form classes of pairs of the binary strings (miRNAs) of the three species human, gorilla and chimpanzee based on Hamming distances 0 to 21 as shown in Table 3. The bar plots with pie plots of these class frequencies are also given the Fig. 6.

For all the three cases of miRNAs of human, gorilla and chimpanzee, none of the clusters with Hamming distances from 0 to 21 is empty. It is also seen that the largest clusters with HD 9 for miRNAs of human, gorilla and chimpanzee contain 1042752, 23076 and 56794 pairs respectively. It interprets that the arrangement of the purine and pyrimidine bases for most of miRNAs of human, gorilla and chimpanzee are differed by 9 bases only.

Classification Based on Distance Pattern of Purine and Pyrimidine

For all the miRNAs of human, gorilla and chimpanzee, the distance patterns between purine bases to the next immediate purine bases are obtained. There are 187, 45 and 64 clusters based on unique distinct patterns of purine bases distance (gap) of miRNAs of human, gorilla and chimpanzee respectively *Additional file-5 (sheet-1,2,3)*. For an example, in the cluster 13 of miRNA of human, the pattern of purine distances in the miRNAs is [1 2 3 4 12] which is interpreted as there are purine bases which are 1, 2, 3, 4 and 12 bases apart. The bar plot of number of miRNAs for the three species human, gorilla and chimpanzee are plotted in Fig. 7.

It is found that most of the miRNAs of human, gorilla and chimpanzee have purine distance patterns [1 2 3] and [1 2 3 4]. There are exactly 553 and 387 many miRNAs of human belong to the cluster 3 ([1 2 3]) and 4 ([1 2 3 4]) respectively. In the case of miRNAs of gorilla, there are 71 miRNAs having purine distance pattern [1 2 3] and 71 miRNAs with distance pattern [1 2 3 4]. For miRNAs of chimpanzee, there are 117 and 116 distance patterns of purine [1 2 3] and [1 2 3 4]. There is no miRNAs of gorilla and chimpanzee having purine distance pattern [1]. In all the three cases, it is noted that there are several clusters having only one member which means that the mirRNA of those clusters has unique purine distance pattern. In the similar fashion, for all the miRNAs of human, gorilla and chimpanzee, the distance between pyrimidine bases to the next immediate pyrimidine bases are found, which is tabulated in the *Additional file-5 (sheet-1,2,3)*. The maximum length of the purine and pyrimidine distance patterns is found to be 5 for all the three set of miRNAs of human, gorilla and chimpanzee except five miRNAs only for human.

We also have determined the frequency distribution of purine and pyrimidine bases of the miRNAs of human, gorilla and chimpanzee as presented in detail in the *Additional file-6*. The clusters based on the frequency distribution of purine is made and tabulated in Table 4. The histogram of frequency distribution of purine bases for the three species are given in Fig. 8.

Classification Based on SEs

For all the miRNAs of the three species human, gorilla and chimpanzee of the Hominidae family, the Shannon entropy is calculated of which detail can be seen in the

bioRxiv preprint doi: https://doi.org/10.1101/208405; this version posted October 24, 2017. The copyright holder for this preprint (which was not certified by peer review) is the author/funder. All rights reserved. No reuse allowed without permission.

Additional file 7. In the case of miRNAs of human, there are exactly 80 distinct SE values are obtained whereas in the case of miRNAs of gorilla and chimpanzee, there are 38 and 57 respectively distinct SEs are found. Based on the Shannon entropy, the miRNAs of the three species are classified into 10 clusters separately as shown in the Table 5. It is observed that most of the miRNAs of all the species human, gorilla and chimpanzee are having Shannon entropy centered at 0.96 which is the largest center of the clusters for all the three different clustering, which contain 1753, 300 and 446 miRNAs respectively. It is seen that there are 16 and 4 miRNAs of human and chimpanzee respectively centered at 0.5 (SE) but there is no member having same center 0.5 in the other set of miRNAs of gorilla. It is also seen that there is no miRNA of human and gorilla, whose Shannon entropy centered at 0.37 but there is only one miRNA of chimpanzee is having SE centered at 0.37. It interprets that none of the miRNAs of gorilla is having equal (approximately) purine-pyrimidine distribution over the sequences whereas there are 16 miRNAs of human which are approximately having random-like purine and pyrimidine distribution. Overall these observations draw an impression that almost none of the miRNAs of all three species is having random-like purine-pyrimidine distribution.

Discussion

The purine and pyrimidine analysis with the binomial distribution shows the purines and pyrimidines are not independently distributed over the miRNAs and there is a tendency of same properties (purine or pyrimidine) to repeat in a miRNA. We found the various classes using different methods where most of the cases the classes are normally distributed although the distribution of the purines and pyrimidines is not random like distribution.

There are 5 miRNAs of human in the cluster 10 based on fractal dimension as shown in the Table-1 having maximum FD. We have seen closely those sequences and found that three of them (h2248, h1954 and h2552) are pyrimidine rich sequences (94%, 90% and 90% respectively) and other two (h1835 and h1291) are purine rich sequence (95% and 100 %) as shown in Table-6. In the case of miRNAs of gorilla and chimpanzee, the cluster 10 contains 2 and 3 miRNAs respectively. Here we convict that whenever the amount of purine or pyrimidine is highly rich in the miRNA sequence then corresponding FD will be maximum.

There are several clusters having miRNAs for human, gorilla and chimpanzee with the same HEs. The frequency distribution of purine and pyrimidine are balanced for all such miRNAs having same HEs. For an example, we took 17 miRNAs from the cluster 7 of miRNAs of human based on Hurst exponent (h463, h526, . . . , h1824 and h2202) which all are having same HE (0.714484) as shown in the Table -7. It is found that the frequency distribution of purine and pyrimidine 60% and 40% (or 40% and 60%) respectively. It is also seen that these 17 miRNAs of human belong to same cluster 3 based on fractal dimension. It is observed that there are 6% miRNAs of human and chimpanzee and 14% miRNAs of gorilla having HE 0.5 which indicates a completely uncorrelated purine and pyrimidine spatial ordering over the miRNAs.

bioRxiv preprint doi: https://doi.org/10.1101/208405; this version posted October 24, 2017. The copyright holder for this preprint (which was not certified by peer review) is the author/funder. All rights reserved. No reuse allowed without permission.

Now we shall see the miRNAs of human having identical distance pattern of purine and pyrimidine. It is observed that there are very few numbers of miRNAs of human which are having identical distance pattern of purine and pyrimidine. For example, h61 miRNA is having identical distance pattern of purine and pyrimidine [1 2]. Also There are miRNAs h36, h51, h62, h83, h122 and h2584 having identical distance pattern of purine and pyrimidine [1 2 3]. There are miRNAs of gorilla g6, g13, g19, g20 and g21 having identical distance pattern of purine and pyrimidine [1 2 3 4]. In the set of miRNAs of chimpanzee, there are p55, p84, p106, p119 and p138 having identical purine and pyrimidine distance pattern. This identical distance pattern of purine and pyrimidine make a guarantee that there are purine and pyrimidine block of same length.

There are 142 distinct frequency distribution of purine and pyrimidine bases across miRNAs of human are found. Out of 2588 miRNAs of human, 194 miRNAs of human having equal frequency distribution of purine and pyrimidine and 1121 miRNAs of human having lesser frequency of purines than that of pyrimidine of 1273 miRNAs are there. This infers frequency of pyrimidine is richer than that of purine over the set of miRNAs of human. On the other hand, there are 43 miRNAs out of 357 miRNAs of gorilla having equal frequency distribution of purine and pyrimidine. There are 58 distinct frequency distribution of purine and pyrimidine bases across miRNAs of gorilla. Out of 357 miRNAs of gorilla, 146 miRNAs of gorilla having lesser frequency of purines than that of pyrimidine of 168 miRNAs are there. There are 92 distinct frequency distribution of purine and pyrimidine bases across miRNAs of chimpanzee are found. Out of 587 miRNAs of human, 67 miRNAs of chimpanzee having equal frequency distribution of purine and pyrimidine and 268 miRNAs of human having lesser frequency of purines than that of pyrimidine of 252 miRNAs are there. This infers frequency of pyrimidine is richer than that of purine over the set of miRNAs of chimpanzee. In this regard we infer that the frequency distribution of pyrimidine over the miRNAs of these three observed species human, gorilla and chimpanzee is richer than that of the purine bases. Out of all the 2588 miRNAs, the miRNA h1291 is only miRNA containing all purine bases.

It is reported that MiR-200 is a family of tumour suppressor miRNAs consisting of five members (h609, h888, h1449, h1677, h1520, h2186, h515, h328 and h670), which are significantly involved in inhibition of epithelial-to-mesenchymal transition (EMT), repression of cancer stem cells (CSCs) self-renewal and differentiation, modulation of cell division and apoptosis, and reversal of chemoresistance [18] as shown in *Table-8*. We have chosen all these nine miRNAs of human including other miRNAs of human which are 0, 1 and 2 Hamming distance apart from those nine miRNAs.

It is found that h888 is 1 Hamming distance apart from h609 and h1520 although h609 and h1520 are 2 Hamming distance apart. The miRNA h888 is having approximately same HD, HE and frequencies of purine and pyrimidine bases with the miRNAs h609 and h1520. Hence we convict that h888 might also work as h609 and h1520 do. It is also observed that h1670 is 2 HD apart from the miRNAs h609

bioRxiv preprint doi: https://doi.org/10.1101/208405; this version posted October 24, 2017. The copyright holder for this preprint (which was not certified by peer review) is the author/funder. All rights reserved. No reuse allowed without permission.

and h515 and the miRNA h1670 is showing very close as per quantitative measures and hence this miRNA h1670 would function as h609 and h515 do. There are two miRNAs of human h1449 and h1677 are 0 Hamming distance apart with same quantitative measures and hence we firmly propose that these two miRNAs would functions same. It is worth noting that both the miRNAs h1449 and h1677 have identical purine-pyrimidine organization. Following the similar argument, other association with the rest of miRNAs can also be made. It is seen that there does not exist any human miRNA which is 0, 1 or 2 HD apart from the miRNA h328.

Concluding Remarks

One of the integral divisions of nucleotides based on their chemical properties is purine-pyrimidine. We attempted to understand the distribution of purine and pyrimidine bases over all the miRNAs in three species human, gorilla and chimpanzee. Quantitatively, we deciphered the self-organization of the purine and pyrimidine bases for all the miRNAs through the fractal dimension of the indicator matrix. Also we took out the auto correlation of purine-pyrimidine bases through the parameter Hurst exponent. To get the nearness of the miRNAs based on their purine-pyrimidine distribution, HD is deployed. The purine-pyrimidine distance patterns including the frequency distribution have been found for all the miRNAs. For all these parameters, we did cluster the miRNAs into several clusters. Based on the quantitative investigation, some crucial observations are adumbrated in the discussion. It is worth noting that through our investigation, the miRNA h1291, made of only purine bases is identified.

Through these investigations what it fails to attain is the association among the miRNAs and target mRNAs as shown in *Table 9*, *Table 10* and *Table 11*. The complex relationship among miRNAs and target mRNAs, previously pointed out in literatures [12] has been reconfirmed through our quantitative analysis over a set of miRNAs and target mRNAs. Imperfect base-pairing between the miRNA and the 3'-UTR of its target mRNA leads to blockage of translation, or at least accumulation of the mRNA's protein product, whereas perfect or near-perfect base-pairing between the miRNA and the middle of its target mRNA causes cleavage of the mRNA, thereby inactivating the same. Such diverse patterns of miRNA action may be responsible for making the correlation among miRNA and target mRNA complex, that are yet to be resolved decisively as pointed out by several researchers earlier. In this context, we plan to bring out the pattern of organization of nucleotides following the other two modes of classifications (amino-keto and strong H-bond and weak H-bond) based on the chemical properties of nucleotides in order to integrate the whole three kinds of grouping to find out the correlationship among the miRNAs-mRNAs and corresponding targeted regions of mRNAs.

Competing interests
The authors declare that they have no competing interests.

Author's contributions
PPC, SSH and AC conceptualize the problem and JKD, SSH and PB performs computational analysis of the datasets. SSH and JKD wrote the manuscript and finally edited and corrected by AC, PB and PPC.

Acknowledgments
The authors acknowledge Prof. R. L. Brahmachary for his valuable suggestions.

bioRxiv preprint doi: https://doi.org/10.1101/208405; this version posted October 24, 2017. The copyright holder for this preprint (which was not certified by peer review) is the author/funder. All rights reserved. No reuse allowed without permission.

Author details

[1]Applied Statistics Unit, Indian Statistical Institute , 203, B. T. Road, West Bengal, 700108 India,. [2]Department of Zoology, Pingla Thana Mahavidyalaya, Maligram, Paschim Medinipur, 722140 Paschim Medinipur, India. [3]Department of Mathematics, Pingla Thana Mahavidyalaya, Maligram, Paschim Medinipur, 722140 Paschim Medinipur, India. [4]International Centre for Theoretical Sciences, TIFR, Bangalore, 560089 Karnataka, India.

References

1. Shi, L., Huang, H.: Dna sequences analysis based on classifications of nucleotide bases. Affective Computing and Intelligent Interaction, 379–384 (2012)
2. Shabarova, Z.A., Bogdanov, A.A.: Advanced Organic Chemistry of Nucleic Acids. John Wiley & Sons, ??? (2008)
3. Watson, J.D., Crick, F.H., *et al.*: Molecular structure of nucleic acids. Nature **171**(4356), 737–738 (1953)
4. Arnott, S., Chandrasekaran, R., Hukins, D., Smith, P., Watts, L.: Structural details of a double-helix observed for dnas containing alternating purine and pyrimidine sequences. Journal of molecular biology **88**(2), 523–45525524533 (1974)
5. He, L., Hannon, G.J.: Micrornas: small rnas with a big role in gene regulation. Nature reviews. Genetics **5**(8), 631 (2004)
6. Li, J., Zhang, Z.: mirna regulatory variation in human evolution. Trends in Genetics **29**(2), 116–124 (2013)
7. Altman, S.: Enzymatic cleavage of rna by rna. Bioscience reports **10**(4), 317–337 (1990)
8. Ambros, V.: The functions of animal micrornas. Nature **431**(7006), 350 (2004)
9. Chen, P.Y., Meister, G.: microrna-guided posttranscriptional gene regulation. Biological chemistry **386**(12), 1205–1218 (2005)
10. Lai, X., Wolkenhauer, O., Vera, J.: Understanding microrna-mediated gene regulatory networks through mathematical modelling. Nucleic acids research **44**(13), 6019–6035 (2016)
11. Enright, A.J., John, B., Gaul, U., Tuschl, T., Sander, C., Marks, D.S.: Microrna targets in drosophila. Genome biology **5**(1), 1 (2003)
12. John, B., Enright, A.J., Aravin, A., Tuschl, T., Sander, C., Marks, D.S.: Human microrna targets. PLoS biology **2**(11), 363 (2004)
13. Stark, A., Brennecke, J., Russell, R.B., Cohen, S.M.: Identification of drosophila microrna targets. PLoS biology **1**(3), 60 (2003)
14. Rajewsky, N.: microrna target predictions in animals. Nature genetics **38**(6s), 8 (2006)
15. Lai, E.C., Tomancak, P., Williams, R.W., Rubin, G.M.: Computational identification of drosophila microrna genes. Genome biology **4**(7), 42 (2003)
16. Mukherji, S., Ebert, M.S., Zheng, G.X., Tsang, J.S., Sharp, P.A., van Oudenaarden, A.: Micrornas can generate thresholds in target gene expression. Nature genetics **43**(9), 854–859 (2011)
17. Jones-Rhoades, M.W., Bartel, D.P.: Computational identification of plant micrornas and their targets, including a stress-induced mirna. Molecular cell **14**(6), 787–799 (2004)
18. Feng, X., Wang, Z., Fillmore, R., Xi, Y.: Mir-200, a new star mirna in human cancer. Cancer letters **344**(2), 166–173 (2014)
19. Volinia, S., Croce, C.M.: Prognostic microrna/mrna signature from the integrated analysis of patients with invasive breast cancer. Proceedings of the National Academy of Sciences **110**(18), 7413–7417 (2013)
20. Iorio, M.V., Ferracin, M., Liu, C.-G., Veronese, A., Spizzo, R., Sabbioni, S., Magri, E., Pedriali, M., Fabbri, M., Campiglio, M., *et al.*: Microrna gene expression deregulation in human breast cancer. Cancer research **65**(16), 7065–7070 (2005)
21. Calin, G.A., Croce, C.M.: Microrna signatures in human cancers. Nature reviews. Cancer **6**(11), 857 (2006)
22. Esteller, M.: Non-coding rnas in human disease. Nature reviews. Genetics **12**(12), 861 (2011)
23. Alshalalfa, M., Alhajj, R.: Using context-specific effect of mirnas to identify functional associations between mirnas and gene signatures. BMC bioinformatics **14**(12), 1 (2013)
24. Muniategui, A., Pey, J., Planes, F.J., Rubio, A.: Joint analysis of mirna and mrna expression data. Briefings in bioinformatics **14**(3), 263–278 (2012)
25. Enerly, E., Steinfeld, I., Kleivi, K., Leivonen, S.-K., Aure, M.R., Russnes, H.G., Rønneberg, J.A., Johnsen, H., Navon, R., Rødland, E., *et al.*: mirna-mrna integrated analysis reveals roles for mirnas in primary breast tumors. PloS one **6**(2), 16915 (2011)
26. Murphy, F.V., Ramakrishnan, V.: Structure of a purine-purine wobble base pair in the decoding center of the ribosome. Nature structural & molecular biology **11**(12), 1251 (2004)
27. Flynt, A.S., Lai, E.C.: Biological principles of microrna-mediated regulation: shared themes amid diversity. Nature reviews. Genetics **9**(11), 831 (2008)
28. Nilsen, T.W.: Mechanisms of microrna-mediated gene regulation in animal cells. TRENDS in Genetics **23**(5), 243–249 (2007)
29. Kozomara, A., Griffiths-Jones, S.: mirbase: annotating high confidence micrornas using deep sequencing data. Nucleic acids research **42**(D1), 68–73 (2013)
30. Cattani, C.: Fractals and hidden symmetries in dna. Mathematical problems in engineering **2010** (2010)
31. Hassan, S.S., Choudhury, P.P., Goswami, A.: Underlying mathematics in diversification of human olfactory receptors in different loci. Interdisciplinary sciences, computational life sciences **5**(4), 270 (2013)
32. Hassan, S.S., Choudhury, P.P., Daya Sagar, B., Chakraborty, S., Guha, R., Goswami, A.: Quantitative description of genomic evolution of olfactory receptors. Asian-European Journal of Mathematics **8**(03), 1550043 (2015)
33. Berthelsen, C.L., Glazier, J.A., Skolnick, M.H.: Global fractal dimension of human dna sequences treated as pseudorandom walks. Physical Review A **45**(12), 8902 (1992)
34. Li, W., Kaneko, K.: Long-range correlation and partial $1/f\alpha$ spectrum in a noncoding dna sequence. EPL (Europhysics Letters) **17**(7), 655 (1992)

bioRxiv preprint doi: https://doi.org/10.1101/208405; this version posted October 24, 2017. The copyright holder for this preprint (which was not certified by peer review) is the author/funder. All rights reserved. No reuse allowed without permission.

35. Arneodo, A., D'Aubenton-Carafa, Y., Audit, B., Bacry, E., Muzy, J., Thermes, C.: What can we learn with wavelets about dna sequences? Physica A: Statistical Mechanics and its Applications **249**(1), 439–448 (1998)
36. Carbone, A., Castelli, G., Stanley, H.E.: Time-dependent hurst exponent in financial time series. Physica A: Statistical Mechanics and its Applications **344**(1), 267–271 (2004)
37. ZuGuo, Y., GuoYi, C.: Rescaled range and transition matrix analysis of dna sequences. Communications in Theoretical Physics **33**(4), 673 (2000)
38. Hamming, R.W.: Error detecting and error correcting codes. Bell Labs Technical Journal **29**(2), 147–160 (1950)
39. Norouzi, M., Fleet, D.J., Salakhutdinov, R.R.: Hamming distance metric learning. In: Advances in Neural Information Processing Systems, pp. 1061–1069 (2012)
40. Burgin, M.: Inductive complexity and shannon entropy. In: Information and Complexity, pp. 16–32 (2017)
41. Zurek, W.H.: Algorithmic randomness and physical entropy. Physical Review A **40**(8), 4731 (1989)
42. Roach, T.N., Nulton, J., Sibani, P., Rohwer, F., Salamon, P.: Entropy in the tangled nature model of evolution. Entropy **19**(5), 192 (2017)
43. Wadsworth, G.P.G.P., Bryan, J.G.: Introduction to probability and random variables. Technical report (1960)

bioRxiv preprint doi: https://doi.org/10.1101/208405; this version posted October 24, 2017. The copyright holder for this preprint (which was not certified by peer review) is the author/funder. All rights reserved. No reuse allowed without permission.

Figures

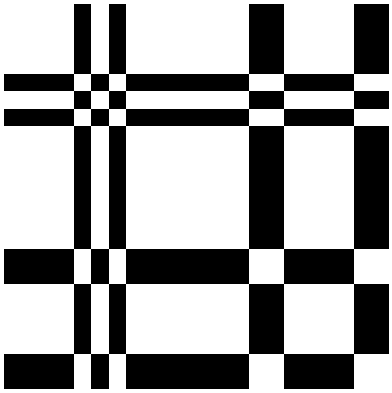

Figure 1 Indicator matrix for the binary sequence $Hsa - miR - 576 - 3pMIMAT0004796$: 11110101111111100111100

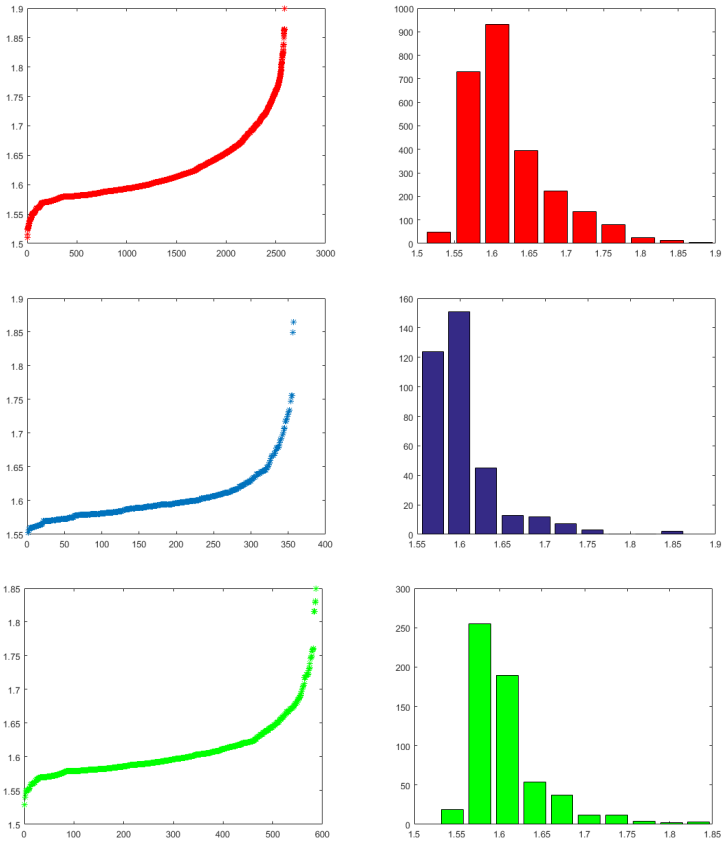

Figure 2 Histograms of fractal dimensions of miRNAs of Human, Gorilla and Chimpanzee from top to bottom respectively.

bioRxiv preprint doi: https://doi.org/10.1101/208405; this version posted October 24, 2017. The copyright holder for this preprint (which was not certified by peer review) is the author/funder. All rights reserved. No reuse allowed without permission.

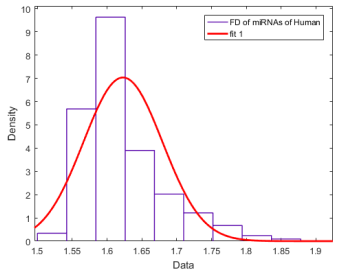

Results:

```
Distribution:    Normal
Log likelihood:  2338.86
Domain:          -Inf < y < Inf
Mean:            1.62892
Variance:        0.00375127

Parameter  Estimate   Std. Err.
mu           1.62892   0.0014846
sigma      0.0612476  0.00105023

Estimated covariance of parameter estimates:
          mu            sigma
mu     2.20404e-06  1.02271e-19
sigma  1.02271e-19  1.10299e-06
```

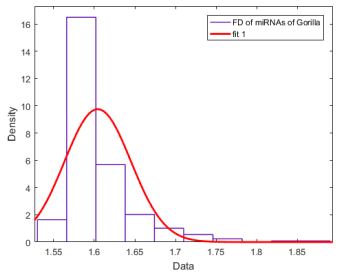

Results:

```
Distribution:    Normal
Log likelihood:  635.135
Domain:          -Inf < y < Inf
Mean:            1.60423
Variance:        0.0016728

Parameter  Estimate   Std. Err.
mu           1.60423   0.00216465
sigma      0.0408999   0.00153387

Estimated covariance of parameter estimates:
          mu            sigma
mu     4.68573e-06  9.52932e-21
sigma  9.52932e-21  2.35275e-06
```

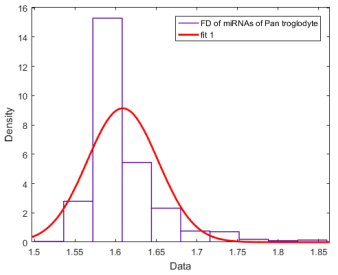

Results:

```
Distribution:    Normal
Log likelihood:  1005.63
Domain:          -Inf < y < Inf
Mean:            1.60868
Variance:        0.00190645

Parameter  Estimate   Std. Err.
mu           1.60868   0.00180216
sigma      0.0436629   0.00127595

Estimated covariance of parameter estimates:
          mu            sigma
mu      3.24778e-06  -1.32745e-19
sigma  -1.32745e-19   1.62805e-06
```

Figure 3 Normal distribution fitting over FDs of miRNAs of Human, Gorilla and Chimpanzee from top to bottom respectively.

bioRxiv preprint doi: https://doi.org/10.1101/208405; this version posted October 24, 2017. The copyright holder for this preprint (which was not certified by peer review) is the author/funder. All rights reserved. No reuse allowed without permission.

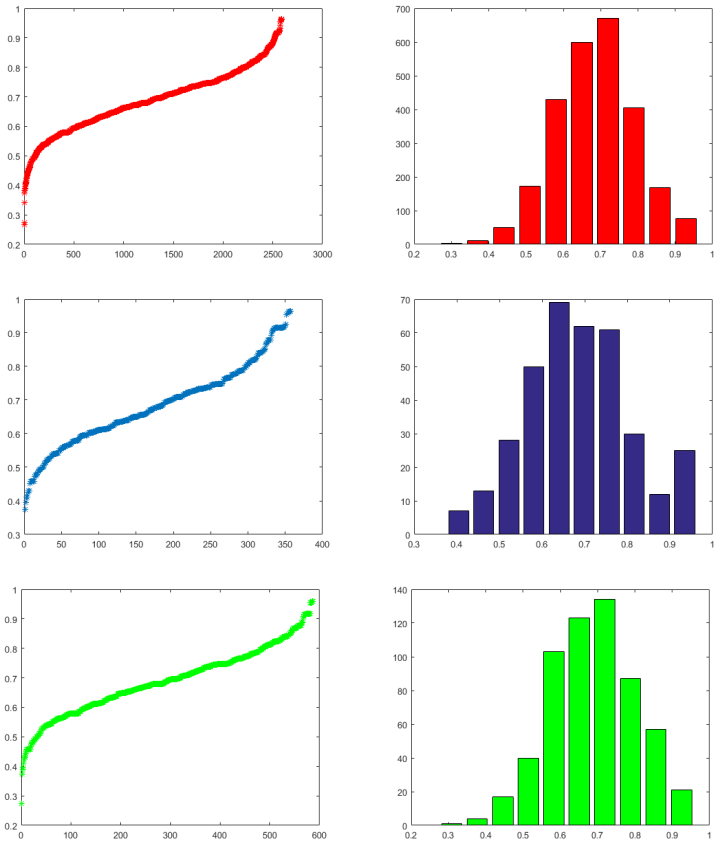

Figure 4 Histograms of Hurst exponents of miRNAs of Human, Gorilla and Chimpanzee from top to bottom respectively.

bioRxiv preprint doi: https://doi.org/10.1101/208405; this version posted October 24, 2017. The copyright holder for this preprint (which was not certified by peer review) is the author/funder. All rights reserved. No reuse allowed without permission.

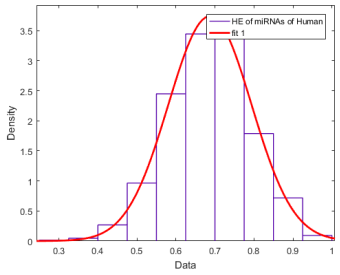

Results:

```
Distribution:    Normal
Log likelihood:  2119.26
Domain:          -Inf < y < Inf
Mean:            0.687211
Variance:        0.0113801

Parameter  Estimate  Std. Err.
mu         0.687211  0.00209737
sigma      0.106678   0.0014835

Estimated covariance of parameter estimates:
       mu            sigma
mu     4.39897e-06   7.13326e-20
sigma  7.13326e-20   2.20076e-06
```

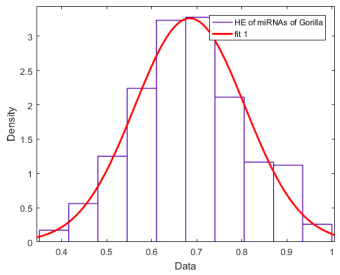

Results:

```
Distribution:    Normal
Log likelihood:  243.909
Domain:          -Inf < y < Inf
Mean:            0.684215
Variance:        0.0149729

Parameter  Estimate  Std. Err.
mu         0.684215  0.00647618
sigma      0.122364    0.004589

Estimated covariance of parameter estimates:
       mu            sigma
mu      4.19409e-05  -8.20072e-20
sigma  -8.20072e-20   2.10589e-05
```

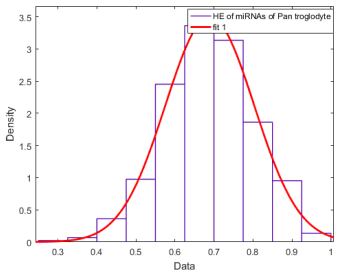

Results:

```
Distribution:    Normal
Log likelihood:  441.245
Domain:          -Inf < y < Inf
Mean:            0.689308
Variance:        0.0130422

Parameter  Estimate  Std. Err.
mu         0.689308  0.00471364
sigma      0.114203  0.00333732

Estimated covariance of parameter estimates:
       mu            sigma
mu      2.22184e-05  -7.31933e-20
sigma  -7.31933e-20   1.11377e-05
```

Figure 5 Normal distribution fitting over HEs of miRNAs of Human, Gorilla and Chimpanzee from top to bottom respectively.

bioRxiv preprint doi: https://doi.org/10.1101/208405; this version posted October 24, 2017. The copyright holder for this preprint (which was not certified by peer review) is the author/funder. All rights reserved. No reuse allowed without permission.

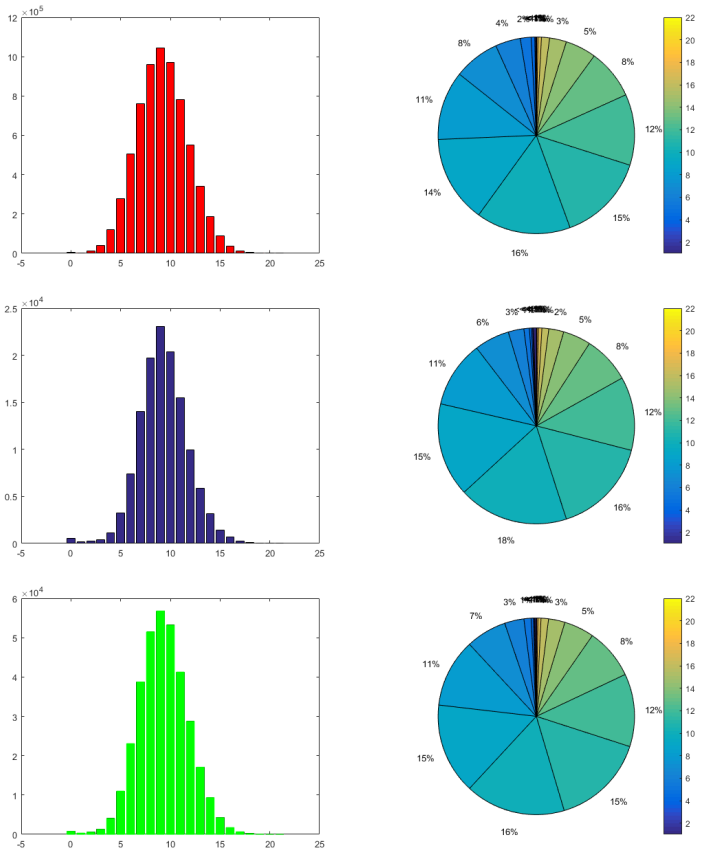

Figure 6 Bar plots and Pie plots of miRNAs of Human, Gorilla and Chimpanzee based on hamming distances from top to bottom respectively.

bioRxiv preprint doi: https://doi.org/10.1101/208405; this version posted October 24, 2017. The copyright holder for this preprint (which was not certified by peer review) is the author/funder. All rights reserved. No reuse allowed without permission.

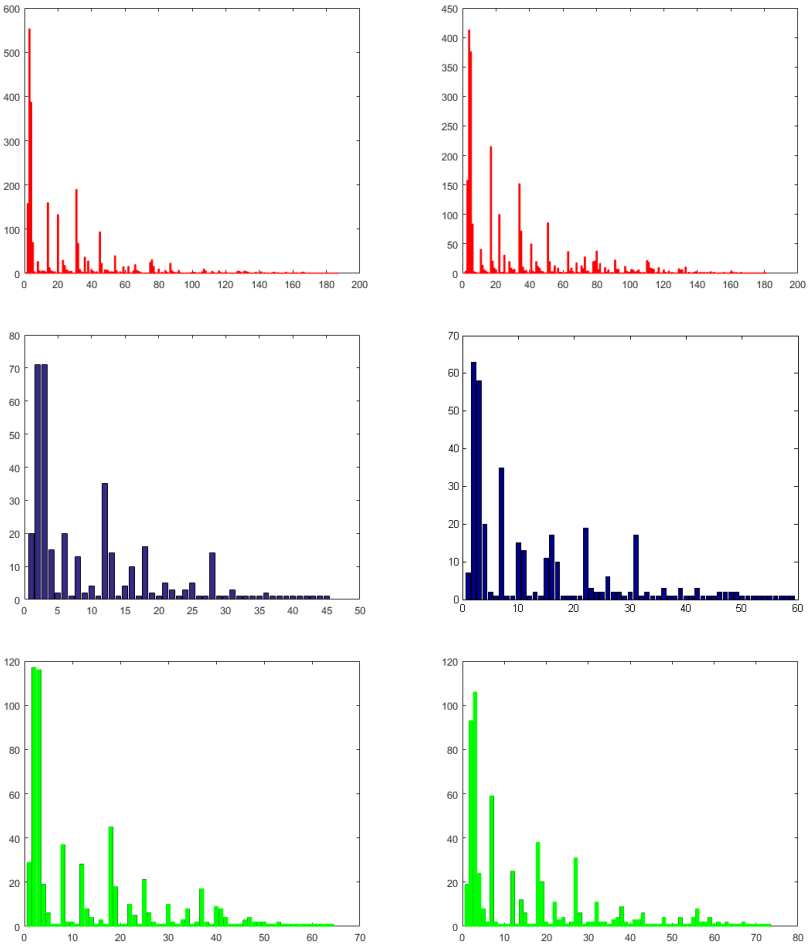

Figure 7 Bar plots of purine (on top) and pyrimidine (on bottom) distances of miRNAs of Human, Gorilla and Chimpanzee from left to right respectively.

bioRxiv preprint doi: https://doi.org/10.1101/208405; this version posted October 24, 2017. The copyright holder for this preprint (which was not certified by peer review) is the author/funder. All rights reserved. No reuse allowed without permission.

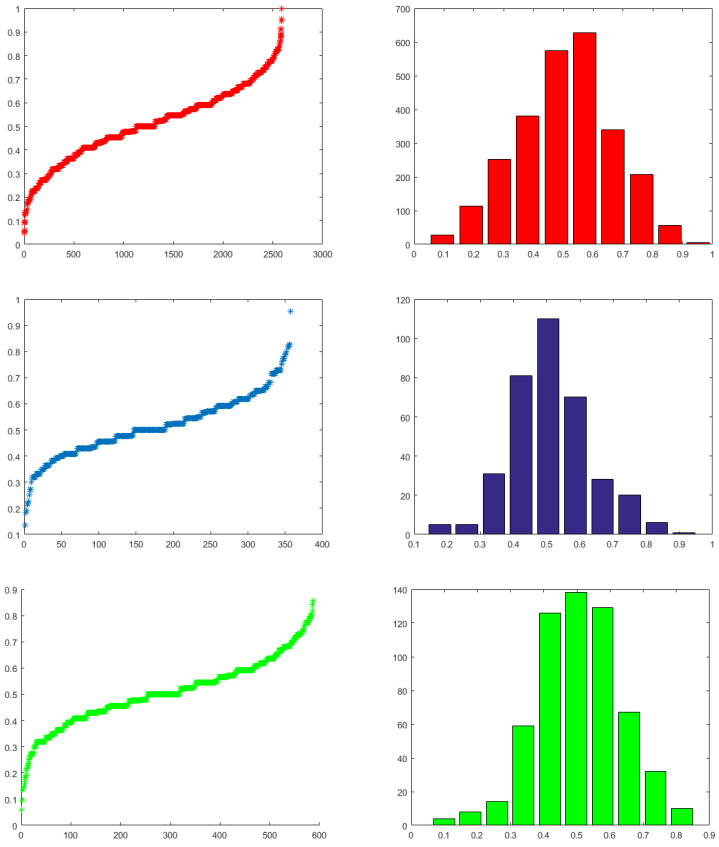

Figure 8 Histograms of frequency distribution of purine bases of the miRNAs of Human, Gorilla and Chimpanzee from top to bottom respectively.

bioRxiv preprint doi: https://doi.org/10.1101/208405; this version posted October 24, 2017. The copyright holder for this preprint (which was not certified by peer review) is the author/funder. All rights reserved. No reuse allowed without permission.

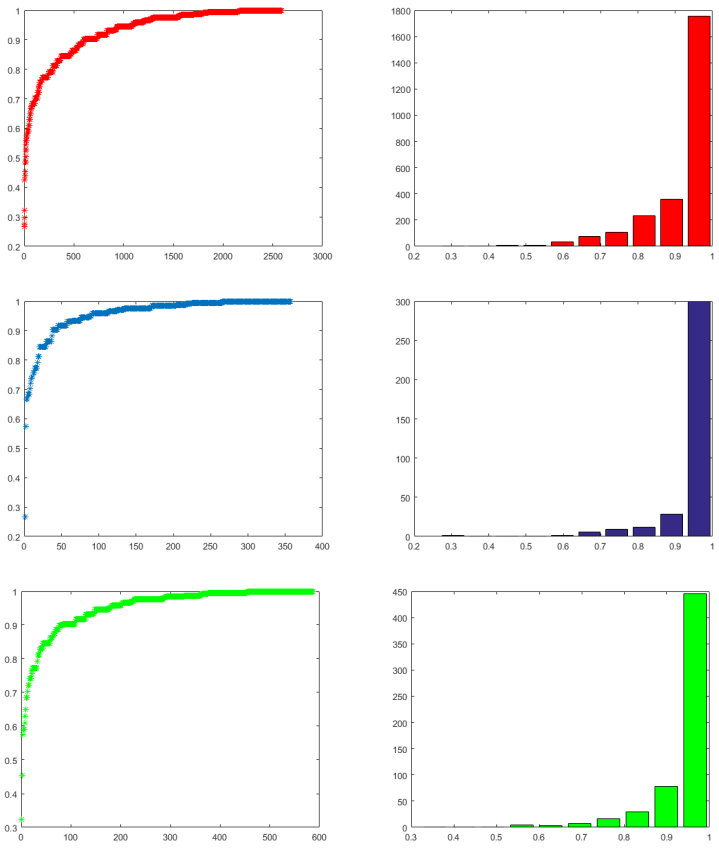

Figure 9 Histograms of Shannon entropy (purine and pyrimidine) Human, Gorilla and Chimpanzee from top to bottom respectively.

bioRxiv preprint doi: https://doi.org/10.1101/208405; this version posted October 24, 2017. The copyright holder for this preprint (which was not certified by peer review) is the author/funder. All rights reserved. No reuse allowed without permission.

Tables

Table 1 Clusters based on Fractal dimension of miRNAs of Human, Gorilla and Chimpanzee.

	Human		Gorilla		Chimpanzee	
Cluster	Frequency	Center	Frequency	Center	Frequency	Center
1	48	1.529	124	1.5683	19	1.5451
2	731	1.568	151	1.5995	255	1.5771
3	931	1.607	45	1.6308	189	1.6092
4	394	1.646	13	1.662	54	1.6413
5	222	1.685	12	1.6932	37	1.6734
6	137	1.724	7	1.7245	12	1.7055
7	80	1.763	3	1.7557	12	1.7375
8	26	1.802	0	1.7869	4	1.7696
9	14	1.841	0	1.8182	2	1.8017
10	5	1.88	2	1.8494	3	1.8338

Table 2 Clusters based on Hurst exponent of miRNAs of Human, Gorilla and Chimpanzee.

	Human		Gorilla		Chimpanzee	
Cluster	Frequency	Center	Frequency	Center	Frequency	Center
1	3	0.3009	7	0.4043	1	0.3087
2	11	0.3707	13	0.4632	4	0.3772
3	50	0.4405	28	0.5221	17	0.4456
4	173	0.5103	50	0.581	40	0.5141
5	430	0.5801	69	0.64	103	0.5825
6	600	0.6499	62	0.6989	123	0.651
7	671	0.7197	61	0.7578	134	0.7194
8	405	0.7895	30	0.8167	87	0.7879
9	168	0.8593	12	0.8756	57	0.8563
10	76	0.9291	25	0.9345	21	0.9248

Table 3 Clusters based on Hamming distance of miRNAs of Human, Gorilla and Chimpanzee. Here number of pairs for each hamming distance is shown, the details cal be seen from Additional files-4.

	Human	Gorilla	Chimpanzee
Distance	Number of pairs	Number of pairs	Number of pairs
0	3768	557	763
1	2602	206	330
2	10620	244	572
3	39956	436	1264
4	119160	1154	4052
5	276592	3274	10996
6	505864	7370	23074
7	760868	14014	38752
8	960910	19714	51488
9	1042752	23076	56794
10	971648	20408	53210
11	781550	15476	41256
12	549660	9930	28722
13	339810	5844	17082
14	186330	3144	9332
15	89458	1444	4244
16	37768	720	1728
17	13404	284	646
18	3918	144	200
19	900	6	54
20	174	2	8
21	32	2	2

bioRxiv preprint doi: https://doi.org/10.1101/208405; this version posted October 24, 2017. The copyright holder for this preprint (which was not certified by peer review) is the author/funder. All rights reserved. No reuse allowed without permission.

Table 4 Clusters based on Frequency distribution (Purine) of miRNAs of Human, Gorilla and Chimpanzee.

	Human		Gorilla		Chimpanzee	
Cluster	Frequency	Center	Frequency	Center	Frequency	Center
1	27	0.0952	5	0.177	4	0.0987
2	114	0.1905	5	0.259	8	0.1786
3	253	0.2857	31	0.341	14	0.2584
4	381	0.381	81	0.423	59	0.3382
5	575	0.4762	110	0.505	126	0.4181
6	628	0.5714	70	0.586	138	0.4979
7	340	0.6667	28	0.668	129	0.5777
8	208	0.7619	20	0.75	67	0.6576
9	57	0.8571	6	0.832	32	0.7374
10	5	0.9524	1	0.914	10	0.8172

Table 5 Clusters based on Shannon entropy of miRNAs of Human, Gorilla and Chimpanzee.

	Human		Gorilla		Chimpanzee	
Cluster	Frequency	Center	Frequency	Center	Frequency	Center
1	5	0.3034	1	0.3034	1	0.3566
2	0	0.3767	0	0.3767	1	0.4243
3	9	0.45	0	0.45	0	0.4921
4	7	0.5233	0	0.5233	4	0.5598
5	35	0.5967	1	0.5967	3	0.6275
6	76	0.67	6	0.67	7	0.6952
7	109	0.7433	9	0.7433	17	0.763
8	233	0.8167	12	0.8167	30	0.8307
9	360	0.89	28	0.89	78	0.8984
10	1753	0.9633	300	0.9633	446	0.9661

Table 6 MiRNAs (from the cluster-10 based on fractal dimension) and its frequency distribution of miRNAs of Human.

Encripted Name	miRNAs sequence	Purine	Pyrimidine
h2248	UGCCCUCCUUUCUUCCCUC	0.053	0.947
h1954	CUUCUCUUCUCUCCUUCCCAG	0.095	0.905
h1835	AAGACGGGAGGAAAGAAGGGAG	0.955	0.045
h2552	UCCUCUUCUCCCUCCUCCCAG	0.095	0.905
h1291	GGGAAAAGGAAGGGGGAGGA	1.000	0.000

Table 7 MiRNAs (from the cluster-7 based on Hurst exponent) and its FD with the frequency distribution of miRNAs of Human.

miRNAs of human	HE	FD	Purine	Pyrimidine
h463	0.714483912	1.611	0.409	0.591
h526	0.714483912	1.608	0.409	0.591
h1655	0.714483912	1.615	0.591	0.409
h1733	0.714483912	1.608	0.591	0.409
h2161	0.714483912	1.612	0.591	0.409
h2219	0.714483912	1.604	0.591	0.409
h262	0.714483912	1.599	0.591	0.409
h515	0.714483912	1.588	0.591	0.409
h747	0.714483912	1.592	0.409	0.591
h782	0.714483912	1.590	0.591	0.409
h1040	0.714483912	1.583	0.409	0.591
h1061	0.714483912	1.583	0.591	0.409
h1240	0.714483912	1.604	0.591	0.409
h1348	0.714483912	1.590	0.591	0.409
h1680	0.714483912	1.586	0.409	0.591
h1824	0.714483912	1.582	0.591	0.409
h2202	0.714483912	1.586	0.409	0.591

bioRxiv preprint doi: https://doi.org/10.1101/208405; this version posted October 24, 2017. The copyright holder for this preprint (which was not certified by peer review) is the author/funder. All rights reserved. No reuse allowed without permission.

Table 8 MiRNAs Star miRNAs in human cancer and their quantifications.

HD	miRNAs	FD	HE	Freq. of Purine	Freq. of Pyrimidine
	h609	**1.579**	**0.578**	**0.5**	**0.5**
HD=1	h888	1.580	0.649	0.545	0.455
HD=2	h515	1.588	0.714	0.591	0.409
HD=2	h875	1.587	0.610	0.478	0.522
HD=2	h1520	1.604	0.627	0.609	0.391
HD=2	h1670	1.579	0.5	0.5	0.5
	h888	**1.580**	**0.649**	**0.545**	**0.455**
HD=1	h515	1.588	0.714	0.5	0.5
HD=1	h609	1.579	0.578	0.5	0.5
HD=2	h1236	1.569	0.654	0.647	0.353
HD=2	h1520	1.604	0.627	0.609	0.391
	h1449	**1.579**	**0.671**	**0.5**	**0.5**
HD=0	h1677	1.579	0.671	0.5	0.5
HD=2	h749	1.509	0.655	0.438	0.563
HD=2	h2186	1.596	0.638	0.409	0.591
	h1677	**1.579**	**0.671**	**0.545**	**0.455**
HD=0	h1449	1.579	0.671	0.5	0.5
HD=2	h749	1.509	0.655	0.438	0.563
HD=2	h2186	1.601	0.638	0.409	0.591
	h1520	**1.604**	**0.627**	**0.609**	**0.391**
Hd=1	h888	1.580	0.649	0.545	0.455
HD=2	h515	1.588	0.714	0.591	0.409
HD=2	h609	1.579	0.578	0.5	0.5
HD=2	h2413	1.590	0.528	0.706	0.294
	h2186	**1.596**	**0.638**	**0.409**	**0.591**
Hd=1	h749	1.509	0.655	0.438	0.563
HD=2	h1449	1.579	0.671	0.5	0.5
HD=2	h1677	1.579	0.671	0.545	0.455
	h515	**1.588**	**0.714**	**0.591**	**0.409**
Hd=1	h888	1.580	0.649	0.545	0.455
HD=1	h1236	1.569	0.654	0.647	0.353
HD=2	h609	1.579	0.578	0.5	0.5
HD=2	h712	1.543	0.745	0.556	0.444
HD=2	h782	1.590	0.714	0.591	0.409
HD=2	h1520	1.604	0.627	0.609	0.391
HD=2	h1670	1.579	0.671	0.5	0.5
	h328	**1.585**	**0.709**	**0.455**	**0.545**
HD=0	×				
HD=1	×				
HD=2	×				
	h1670	**1.579**	**0.671**	**0.5**	**0.5**
Hd=2	h515	1.588	0.714	0.591	0.409
HD=2	h609	1.579	0.578	0.5	0.5
HD=2	h2485	1.533	0.873	0.471	0.529

Table 9 Selected miRNAs of Human and the corresponding target mRNAs.

Sl no.	miRNAs	Encripted Name	Target mRNAs	Encripted Name	Disease
1	hsa-mir-143	h508	ERK5	t1	Obesity
2	hsa-mir-20a	h203	TGFBR2	t2	Breast Neoplasms
3	hsa-mir-16-1	h907	BCL2	t3	Leukemia, Lymphocytic, Chronic, B-Cell
4	hsa-mir-221	h1310	KIT	t4	Thyroid Neoplasms
5	hsa-mir-15a	h1637	BCL2	t3	Leukemia, Lymphocytic, Chronic, B-Cell
6	hsa-mir-146a	h76	KIT	t4	Thyroid Neoplasms
7	hsa-mir-200a	h185	RAB30	t5	Carcinoma, Hepatocellular
8	hsa-mir-103a-2	h37	DMPK	t6	Myotonic Dystrophy
9	hsa-mir-29a	h1178	DNMT3A	t7	Lung Neoplasms
10	hsa-mir-29b-1	h809	DNMT3A	t7	Lung Neoplasms
11	hsa-mir-185	h892	DNMT3A	t7	Glioma
12	hsa-mir-590	h1188	TGFBR2	t2	Carcinoma, Hepatocellular
13	hsa-mir-106a	h288	TGFBR2	t2	Colorectal Neoplasms

bioRxiv preprint doi: https://doi.org/10.1101/208405; this version posted October 24, 2017. The copyright holder for this preprint (which was not certified by peer review) is the author/funder. All rights reserved. No reuse allowed without permission.

Table 10

Target mRNAs	FD	HE	Purine distance pattern	Pyrimidine distance pattern
t1	1.94	0.6634044	[1 2 3 4 5 6 7 8 9 10 11]	[1 2 3 4 5 6 7 8 9 10 12 13]
t2	1.89362	0.5792666	[1 2 3 4 5 6 7 8 9 10]	[1 2 3 4 5 6 7 8 10 11 17]
t3	1.8819	0.6976582	[1 2 3 4 5 6 7 8 9 11 13 17]	[1 2 3 4 5 6 7 8 9 10 11]
t4	1.92328	0.6255126	[1 2 3 4 5 6 7 8 9 10 12 13 15]	[1 2 3 4 5 6 7 8 9 10 11 12 14 16 18]
t5	1.8773	0.5928585	[1 2 3 4 5 6 7 8 10 13]	[1 2 3 4 5 6 7 8 9 14 15]
t6	1.90762	0.7073991	[1 2 3 4 5 6 7 8 9 10 12 13 14]	[1 2 3 4 5 6 7 8 9 10 12 14 19]
t7	1.91941	0.6735526	[1 2 3 4 5 6 7 8 9 10 11 12]	[1 2 3 4 5 6 7 8 9 10 11 12 13 16]

Table 11 MiRNAs of Human and Corresponding Quantifications

Sl no.	miRNAs	Encripted Name	FD	HE	Purine distance pattern	Pyrimidine distance pattern
1	hsa-mir-143	h508	1.5938	0.7456	[1 2 3]	[1 2 3 5]
2	hsa-mir-20a	h203	1.795	0.6331	[1 2 3 4]	[1 2 4]
3	hsa-mir-16-1	h907	1.5845	0.4723	[1 2 3]	[1 2 3]
4	hsa-mir-221	h1310	1.6117	0.5402	[1 2 3 4]	[1 2 4]
5	hsa-mir-15a	h1637	1.5999	0.5755	[1 2 3 5]	[1 2 4]
6	hsa-mir-146a	h76	1.5850	0.6804	[1 2 3 5]	[1 2 4 6]
7	hsa-mir-200a	h185	1.5794	0.6711	[1 2 3 5]	[1 2 3 4]
8	hsa-mir-103a-2	h37	1.6432	0.6680	[1 2 3 5]	[1 2 3]
9	hsa-mir-29a	h1178	1.6460	0.7505	[1 2 3 4]	[1 2 3]
10	hsa-mir-29b-1	h809	1.5976	0.5578	[1 2 3 4]	[1 2 3]
11	hsa-mir-185	h892	1.6501	0.8410	[1 2 6]	[1 3 12]
12	hsa-mir-590	h1188	1.5835	0.7962	[1 2 4]	[1 2 3 6]
13	hsa-mir-106a	h288	1.5843	0.7666	[1 2 7]	[1 2 3 4]

bioRxiv preprint doi: https://doi.org/10.1101/208405; this version posted October 24, 2017. The copyright holder for this preprint (which was not certified by peer review) is the author/funder. All rights reserved. No reuse allowed without permission.

Additional Files

Additional file 1 — Name Encryption of miRNA of Human, Gorilla and Chimpanzee.

Additional file 2 — Fractal Dimension (FD) of all binary sequences of Human, Gorilla and Chimpanzee (sheet-1) and the detail members (miRNAs) of the clusters for Human, Gorilla and Chimpanzee based on FD (sheet-2).

Additional file 3 — Hurst Exponent (HE) of all binary sequences of Human, Gorilla and Chimpanzee (sheet-1) and The detail members (miRNAs) of the clusters for Human, Gorilla and Chimpanzee based on HE (sheet-2).

Additional file 4 — The Hamming Distance (HD) matrices of (miRNAs) of Human (sheet 1), Gorilla (sheet 2) and Chimpanzee (sheet 3) between the pair of two sequences which can be identified by the corresponding row and column numbers.

Additional file 5 — The detail clustering of miRNAs of Human (sheet 1), Gorilla (sheet 2) and Chimpanzee (sheet 3) with cluster numbers based on the immediate purine and pyrimidine distances as patterns.

Additional file 6— The detail frequency distribution of purine and pyrimidine of miRNAs of Human, Gorilla and Chimpanzee.

Additional file 7— Shannon Entropy (SE) of all binary sequences of Human, Gorilla and Chimpanzee (sheet-1 and the detail members (miRNAs) of the clusters for Human, Gorilla and Chimpanzee based on SE (sheet-2).